Mechanical-Based Design for Airfoil Structural Morphing

Mattia Butera*, Amanda Butler*, Amiri Hayes*, Evan Schaffer*, Niti Sinha*
Jay Kapasiawala† and Dr. Prosenjit Bagchi†
*The New Jersey Governor's School of Engineering and Technology, Rutgers University–New Brunswick, NJ, USA
†Corresponding Author
Emails: {mattia.t.butera, fofochiab, amirihayes1, evankschaffer, nitisinha0829}@gmail.com
{jk1695@rutgers.edu, pbagchi@soe.rutgers.edu}

***Abstract*—Airfoils are designed to perform optimally at a specific flight regime. Inefficient flight is caused when a fixed geometry is used at both supersonic and subsonic speeds, speeds that are above and below the speed of sound respectively. Supersonic airfoils do not generate enough lift to be used effectively at subsonic speeds and subsonic airfoils generate more drag than lift at supersonic speeds. The ideal airfoil maximizes lift while minimizing drag. A prototype that changes airfoil geometry mid-flight was thus constructed, tested using computer simulations (Ansys and COMSOL), and proven with aerodynamic equations, revealing the effectiveness of a morphing airfoil in multiple flight step filet regimes.**

I. Introduction

A. Overview

The rapid modernization of the aviation industry has incited widespread interest in aircraft with the ability to achieve supersonic speeds. The notion of improved performance and sustainability has incentivized manufacturers to design aircraft which can fly at supersonic speeds without deleterious effects on fuel efficiency, noise pollution, or smog. While subsonic speeds are considerably easier to design around, the aircraft industry intends to progress towards a future with reduced flight time and emissions.

B. Motivation

If the wing geometry is inappropriate for the flight regime, as the aircraft approaches supersonic speeds, drag divergence–where the force (drag) that prevents flight increases rapidly–occurs. Contrary to supersonic airfoils, airfoils designed to maximize lift in subsonic flight are generally thicker and rounder, which forms an intense shockwave at supersonic speeds and an increased amount of flow separation, increasing drag and decreasing efficiency [1]. Hence, subsonic and supersonic aircraft are two separate categories and require distinct airfoil geometries. For aircraft to traverse these flight regimes efficiently, a mid-flight modification of the airfoil is required. Computer simulations, principle aerodynamics calculations, and construction of an airfoil prototype with dynamic geometry were successfully implemented in this design for an amorphous airfoil.

II. Background

A. Aerodynamic Efficiency

An airfoil is a two-dimensional representation of the cross-sectional area of an aircraft wing. Lift and drag are the two main forces influencing flight; lift enables flight while drag resists it. The coefficients of lift and drag are non-dimensionalized values derived from lift and drag.

Lift, the upward force exerted on the wing, opposes the downward gravitational force and allows for flight. For airfoils, the lift force L is equal to the product of the air density ρ, the velocity v, and the air circulation Γ.

$$L = \rho V_\infty \Gamma \tag{1}$$

How much lift an airplane can generate depends on the wing geometry, which includes the chord length, angle of attack, camber, shape of the wing, and ratio of the wing span to wing area.

Drag is a force which is exerted horizontally towards the rear of the airfoil, opposing forward motion. Induced drag, caused by downwash (the downward diversion of the incoming airstream caused by an aircraft wing), is the most important type of drag to consider in aerodynamics at both subsonic and supersonic speeds [1]. At supersonic speeds, the friction due to air viscosity (a fluid's resistance to flow) increases, causing wave drag. Flow separation causes a section of recirculating air with low velocity above the wing. As a result of Bernouli's principle, increased pressure above the wing is created, resulting in wave drag.

$$D_i = L \sin \alpha_i \tag{2}$$

Equation (2) describes drag force as a function of lift force L and the angle of attack α. Using these values of lift and drag, coefficients of lift and drag were then calculated.

$$c_L = \frac{L}{\frac{1}{2}\rho V_\infty l} \tag{3}$$

$$c_D = \frac{D}{\frac{1}{2}\rho V_\infty l} \tag{4}$$

Lift and drag are correlated; as lift increases, drag increases. When the speed of an airplane is slower than the speed of sound (343 m/s), it is optimal for the shape of the airfoil to resemble an asymmetric, horizontal teardrop (see Figure 3). At supersonic speeds, the shape of the airfoil must be thinner, which sacrifices lift, but decreases a significant amount of drag [1].

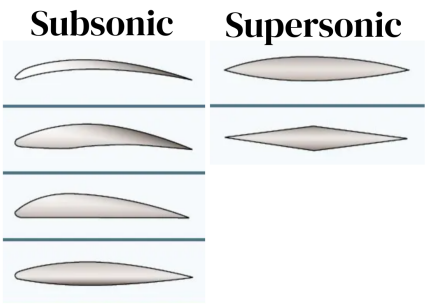

Fig. 1. Subsonic Airfoil Geometry Versus Supersonic Airfoil Geometry [5-6]

Another essential factor to consider is the Angle of Attack (AOA). Increasing the AOA generally increases lift as well as induced drag. This trend only continues until 15-20 degrees, at which point lift is lost because airflow across the upper side of the airfoil becomes detached in an event known as stall. It is essential to obtain a proper AOA which maximizes lift without causing stall [7]. Simulations for this paper were conducted at a 10-degree AOA.

B. Quantifying Lift and Drag

A static airfoil that is optimized for subsonic flight is not fit for supersonic flight and vice versa [8]. In order to calculate values of lift and drag to confirm this, simulations in COMSOL and Ansys were used. An airfoil that can morph efficiently would get thinner as speed increases and would take advantage of increasing values of lift from thinner airfoils in the supersonic regime.

C. Existing Research

Currently, almost all aircraft are designed to perform most efficiently only within a specific environment. Creating a mechanism in which the airfoil shape could morph would overcome these issues to create a more versatile aircraft. Existing solutions that have been developed include the use of shape memory alloys (SMAs) and machinery which twists, bends, or rotates the wing. SMAs are metals or alloys which are purposefully deformed and can return to their original state when heated [10]. The other type of morphing proposed is machinery inside the wing, which often employ motor-based systems. Both of these solutions have been implemented only in prototypes.

III. Procedure

A. A Mechanical Approach

To allow for a more efficient flight, a morphing airfoil with changing geometry was constructed. A design with a cam system driven by a NEMA-17 stepper motor was selected; a cam converts rotational motion, in this case from the stepper motor, into linear motion. The flexible material for the airfoil was selected to be fiberglass in combination with epoxy so that the rotation of the cam would allow the geometry of the airfoil to change.

B. Comsol, Ansys and MATLAB

The two softwares used to create computer simulations for airfoils were COMSOL Multiphysics and Ansys. These are ideal platforms that use computational fluid dynamics to model airfoils; they return values such as lift force (L) and drag force (D) and are capable of generating pressure and velocity graphs. These values were also calculated individually using MATLAB to introduce another layer of accuracy.

C. Employing COMSOL and ANSYS

1) COMSOL: COMSOL software was implemented to simulate subsonic flight. The extended set of points that makes up the airfoil point-curve was found online at Airfoil Tools and imported as an interpolation curve using a table. *Laminar Flow simulation* was selected to input the necessary parameters and aerodynamic equations into the software. Parameters for pressure, velocity, temperature, and AOA were specified, and simulation was generated. Further, tables were generated by specifying quantities (such as lift force) to calculate. It is important to note that subsonic speed simulations were created in COMSOL due to the software being more effective for this flight regime than Ansys [1].

2) ANSYS: Supersonic flight was simulated in CFD software, Ansys. A *.STEP* file of the desired airfoil geometry was imported into the geometry of an Ansys Fluid Flow (fluent) file. After the geometry was edited and a mesh was created, a viscous model was created in a density based simulation. The environmental conditions were set to Mach number 3.5, temperature 242 K and pressure 54,000 Pa [12]. After initializing the simulations, calculations were specified to generate specified quantities (such as lift and drag forces), along with a pressure contour graph.

3) MATLAB: After simulating the airfoils, MATLAB was used to calculate the coefficients of lift and drag. Aerodynamic equations were employed which declared lift as a function using the following equations:

$$c_L = 2\pi(1 + \frac{4}{3\sqrt{3}})(\frac{t}{l})\alpha \tag{5}$$

$$c_D i = \frac{L\alpha}{\frac{1}{2}\rho v^2 l} \tag{6}$$

$$c_D f = \frac{D_f}{\frac{1}{2}\rho v^2 l} \tag{7}$$

where α is AOA in radians, t is the max thickness of the airfoil in meters, h is the max camber in meters, l is the chord length in meters, v is free stream velocity in meters per second, $/rho$ is air density in grams per cubic meter, D is drag in Newtons, and L is lift in Newtons. The values for L and D are derived from Equations (1) and (2). The coefficients of lift and drag were calculated using the code in Appendix A: `Lift & Drag Calculations`, graphed, and compared with the simulated values at multiple angles of attack to corroborate information about the efficiency of the airfoil.

In addition, fuel efficiency for considered airfoils was calculated to confirm that the amorphous design was more sustainable than non-morphing airfoils. Calculating the fuel efficiency ensures that the weight of the aircraft as a whole—including the motor, cam, and other components—still demands less fuel than current alternatives. Fuel efficiency was calculated using the following kinematic equations which can be found in Appendix B:

$$D = \frac{c_D \rho v^2 A_1}{2} \tag{8}$$

$$L = \frac{c_L \rho v^2 A_2}{2} \tag{9}$$

where v is the velocity of the aircraft, A_1 is the cross sectional area of the airfoil, and A_2 is the planform area of the wing. It is important to note that lift and drag in Equations (8) and (9) are for the entire aircraft rather than solely the airfoil. The aircraft's lift, drag, thrust and weight at supersonic and subsonic speeds was then used in kinematic equations to determine the number of gallons consumed per mile.

D. Final Airfoil Model

The airfoil of the subsonic P-51 Mustang, the BL17.5, was chosen because of its lesser thickness (16.5%). The airfoil of the supersonic F-16 Fighting Falcon, the NACA 64-206, was also chosen due to its similar dimensions to the subsonic airfoil [15-16]. [17-18]. The airfoils were proportioned to one another according to their perimeters. The final model preserved the same surface area but changed thickness, camber, and chord length.

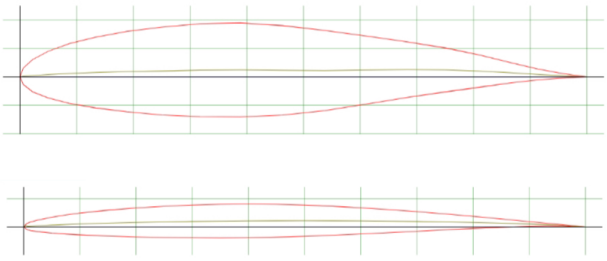

Fig. 2. (top) BL17.5 subsonic and (bottom) NACA 64-206 supersonic airfoils [17-18]

The prototype was constructed by employing 3D printing and laser cutting, and built with materials such as fiberglass and epoxy. Despite an airfoil being a two-dimensional representation of an airplane wing, the physical prototype contains necessary internal structure to provide depth to create a wing (see figure 10). The width of the elliptical cam would correspond to the supersonic airfoil thickness, and the height to the subsonic airfoil thickness (see figure 6). To provide structure to the trailing edge, a connecting rod was anchored at a point on the cam; as the airfoil thickened, the chord length of the airfoil diminished.

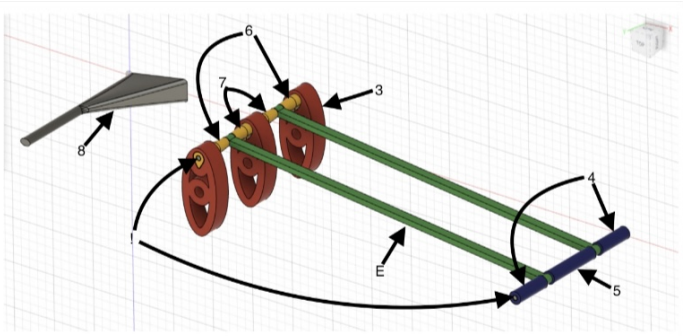

Fig. 3. Fusion 360 Cam System

TABLE I
AIRFOIL DIMENSIONS

	BL17.5	NACA 64-206
Aircraft	p-51	F-16
Chord length [m]	0.35	0.335164
Max thickness [% of chord]	16.5	6
M.T. location [% of chord]	38.9	40
Max thickness[m]	0.05775	0.020109
M.T. location [m]	0.13615	0.134065
Max camber [% of chord]	1.3	1.1
M.C. location [% of chord]	68.3	50
Max camber [m]	0.00455	0.003687
M.C. location [m]	0.23905	0.167582

IV. RESULTS

A. Physical Airfoil Performance

The final physical airfoil was composed of the cam mechanism, the fiberglass-epoxy airfoil, and an acrylic, laser-cut baseboard to house the stepper motor. The stepper motor and circuit successfully rotated the cam 90 degrees counterclockwise from the vertical (subsonic) position to the horizontal (supersonic) position. The fiberglass-epoxy combination flexed with the movement of the cam. The cam mechanism changed the chord length, thickness, and camber of the airfoil, demonstrating the viability of an amorphous airfoil.

B. Simulation Proof

COMSOL and Ansys simulations each used typical flight environments. Atmospheric pressure was standardized across experiments at a constant 54000 Pa, and atmospheric temperature was standardized at a constant 242K, or -31.15 degrees Celsius [12]. These parameters model ideal passenger flight conditions. Subsonic simulations were tested at 100 m/s, well within the subsonic range and well below the transonic flow region, which begins at Mach 0.8 (274.4 m/s). Similarly, supersonic simulations were tested at Mach 3.5 (1200.5 m/s), well above the supersonic and transonic flow cutoff, which ends at about Mach 1.2 (411.6 m/s). The AOA was also standardized at ten degrees, though data was collected at zero degrees as well.

1) BL17.5 Simulations: Figure 17 demonstrates the BL17.5 at subsonic speed with a 10 degree AOA. When tested in COMSOL at 100 m/s, the BL17.5 airfoil generated 1147.46%

greater lift force than the generated drag force of 208.54 N (see Table 3). Airstream velocity at the upper leading edge was much greater than below the airfoil, generating lift.

TABLE II
BL17.5 VALUES FROM SIMULATION AND CALCULATION

BL17.5	AOA	100[m/s]	Mach 0.6	Mach 3.5
chord length [m]		1.0	1.0	1.0
lift force [N]	0	-529.46	-2251	-
	10	2348.40	10001	-
drag force [N]	0	287.06	1215.1	-
	10	695.61	2943.20	-
Coefficient of Lift	0	-0.09	-0.06	-
	10	0.38	0.26	-
Coefficient of Drag	0	0.05	0.03	-
	10	0.11	0.08	-

The BL17.5 airfoil would be ineffective at supersonic speeds because it would generate a high amount of wave drag. The thickness of the BL17.5 is too great for supersonic speeds; the most optimal airfoil found was the NACA 64-206 [21].

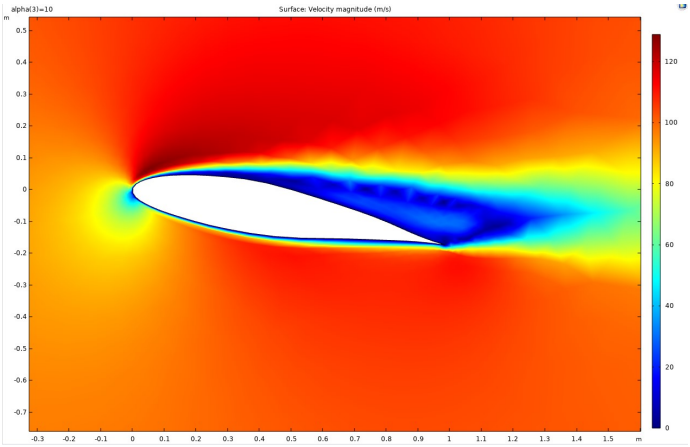

Fig. 4. BL17.5 with 10 degree AOA at 100m/s (from COMSOL)

2) NACA 64-206 Simulations: When tested in Ansys at Mach 3.5 (see figure 21), the NACA 64-206 airfoil generated 368.6% greater lift force than the generated drag force of 637928.3 N (see Table 3). The highest pressure is visible below the airfoil, while the lowest is visible above the airfoil; this generates lift. The triangular contour displays the existence of a shockwave, which is inevitable at supersonic speeds. When tested in COMSOL at 100 m/s (see figure 20), the NACA 64-206 generated a significantly smaller force of lift (3693.8 N), compared to the corresponding supersonic lift force (2351798 N) (see Table 3). Drag force of the NACA 64-206 followed a similar pattern. The NACA 64-206 was most effective at supersonic speeds.

C. Matlab

The coefficients of lift and drag were simultaneously calculated in MATLAB with aerodynamics equations (4), (5), and (6). `Lift & Drag Calculations` graphed the simulation and obtained values for coefficient of lift and coefficient of friction against simulation obtained values. Theoretical values

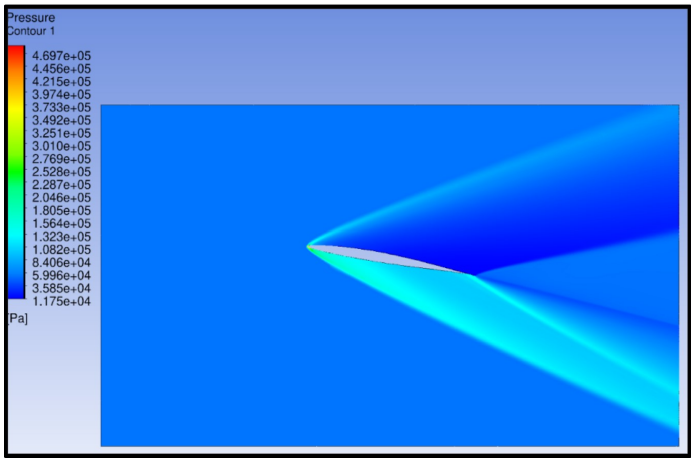

Fig. 5. NACA 64-206 at Mach 3.5 with 10 degree AOA

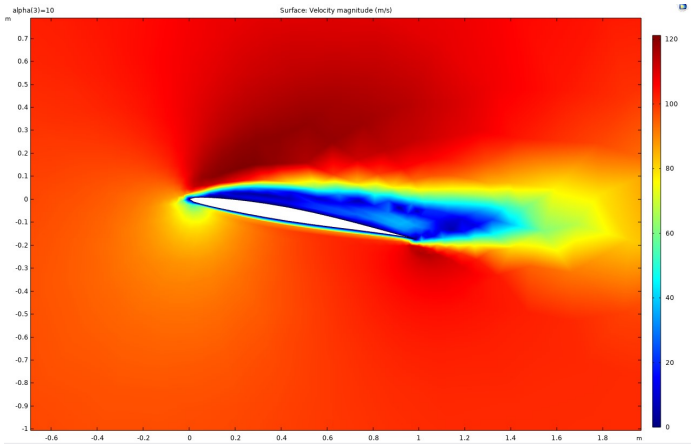

Fig. 6. NACA 64-206 at 100[m/s] with 10 degree AOA

were generally higher than experimental values. Nevertheless, the data clearly showed that higher values for lift and lower values for drag were achieved with the two airfoils used in the morphing design.

Additionally, the fuel consumption graphs showed that the BL 17.5 and NACA 64-206 airfoils used less fuel when the wing changed from one to the other. Employing `Fuel Efficiency Calculations`, data was collected about the aircraft the morphing wing would be attached to and used to approximate the fuel efficiency. Then the morphing aircraft was compared to the P51 and F-16 planes which use the Bl 17.5 and NACA 64-206 airfoils to determine which was more fuel efficient. Despite the weight and relative added complexity introduced to the aircraft by the morphing airfoil, the morphing design saved about 0.522 gallons of JP-8 jet fuel per mile.

V. CONCLUSIONS

A. Accomplishments and Significance of Findings

The COMSOL and Ansys simulations demonstrated the effectiveness of airfoils in their respective Mach environments. This disparity in airfoil effectiveness demonstrated the value of

TABLE III
NACA 64-206 VALUES FROM SIMULATION AND CALCULATION

NACA 64-206	AOA	Mach 0.3	Mach 0.6	Mach 3.5
chord length [m]		1.0	1.0	1.0
lift force [N]	0	329.40	1395.4	-18373.64
	10	3747.4	15828	2351798
drag force [N]	0	36.60	154.76	28751.1
	10	803.67	3396.00	637928.30
Coefficient of Lift	0	0.05	0.05	-0.00083
	10	0.06	0.06	0.11
Coefficient of Drag	0	0.01	0.01	0.01
	10	0.13	0.13	2.65

an amorphous airfoil. The physical model demonstrated that such a transitioning airfoil could be achieved with a simple mechanical process and lift/drag tests proved the extent to which this transition would improve efficiency. The employment of amorphous airfoils would be invaluable to maximize efficiency in multiple environments. With this proof of concept design, the developed morphing airfoil experienced increased lift in subsonic environments and decreased drag in supersonic environments caused by the change in airfoil geometry.

B. Future Research

The physical model of the amorphous airfoil could be improved with alternative resources. A stronger and more flexible material such as a Kevlar mixed with epoxy could expand the mechanical limits of the transition system [9]. Furthermore, aerodynamic factors such as drag on the material of the wing surface and varying airfoil thickness along the wing could be considered. Future research could experiment with different airfoil geometries. More extensive optimization techniques could be used to determine additional mechanism shapes.

VI. ACKNOWLEDGMENTS

The authors of this paper would like to thank those who allowed this research project to be successful: the Rutgers School of Engineering, Rutgers University, and the State of New Jersey Office of the Secretary of Higher Education for giving us the opportunity for further education in engineering; Lockheed Martin and other sponsors for generously funding our projects, and Governor's School of New Jersey Program in Engineering and Technology alumni and benefactors for their support and participation. It is also imperative to thank Dean Jean Patrick Antoine, Director of Governor's School of New Jersey Program in Engineering and Technology, for his management and supervision; Project Mentor Jay Kapasiawala for his fundamental teaching and guidance; Dr. Prosenjit Bagchi, MAE Professor of Rutgers University School of Engineering, for his counseling; Residential Teaching Assistant Lasya A. Balachandran for her vital time and assistance; Research Coordinator June Lee for her support; Head Residential Teaching Assistant Ian Joshua C. Origenes for his supervision and management, and members of the Rutgers Makerspace for their invaluable aid in constructing the physical model.

REFERENCES

[1] J. Kapasiawala, "Amorphous Airfoil Design," Jun. 2022.
[2] "NASA Fundamental Aeronautics Student Competition Technical Area: Supersonic Flight Project." [Online]. Available: https://www.nasa.gov/sites/default/files/atoms/files/2008-2009-1st-non-us-tea 3_kareas.pdf
[3] Acoustics.org, 2022. https://acoustics.org/wp-content/uploads/2019/12/Figure_01_Airplane_Sketch-1024x714.jpg
[4] Ifatceg.com, 2022. https://ifatceg.com/wp-content/uploads/2021/06/B628DCC8-5D31-4BD4-B748-0332C6A8020D.png (accessed Jul. 19, 2022).
[5] P. of Flight, "Airfoil Design (Part One)," Flight Literacy, Nov. 27, 2017. https://www.flightliteracy.com/airfoil-design-part-one/
[6] R. Kolluru and V. Gopal, "Numerical Study of Navier-Stokes Equations in Supersonic Flow over a Double Wedge Airfoil using Adaptive Grids Hybrid Optimization algorithms View project NOVEL Algorithms for Compressible flows View project Numerical Study of Navier-Stokes Equations in Supersonic Flow over a Double Wedge Airfoil using Adaptive Grids."
[7] Skybrary, "Angle of Attack (AOA)," SKYbrary Aviation Safety, May 25, 2021. https://skybrary.aero/articles/angle-attack-aoa
[8] K. M. Casper, J. Wagner, S. J. Beresh, J. F. Henfling, R. W. Spillers, and B. O. M. Pruett, "Complex Geometry Effects on Subsonic Cavity Flows.," www.osti.gov, Dec. 01, 2014. https://www.osti.gov/servlets/purl/1242764 (accessed Jul. 22, 2022).
[9] T. F. Geyer and E. Sarradj, "Trailing Edge Noise of Partially Porous Airfoils," 20th AIAA/CEAS Aeroacoustics Conference, Jun. 2014, doi: 10.2514/6.2014-3039.
[10] M. Cho and S. Kim, "Structural morphing using two-way shape memory effect of SMA," International Journal of Solids and Structures, vol. 42, no. 5–6, pp. 1759–1776, Mar. 2005, doi: 10.1016/j.ijsolstr.2004.07.010
[11] "DARPA Smart Wing Program arph59bg3n2," 2004. Accessed: Jul. 16, 2022. [Online]. Available https://mipt.ru/education/chairs/theor_cyberneticsgovernment/upload/77e/DARPA_Smart_Wing_Program-arph59bg3n2.pdf
[12] "X-15 Research Results: Chapter 5," history.nasa.gov. https://history.nasa.gov/SP-60/ch-5.html
[13] "North American P-51 Mustang — The National WWII Museum — New Orleans," The National WWII Museum — New Orleans, 2019. https://www.nationalww2museum.org/visit/museum-campus/us-freedom-pavilion/warbirds/north-american-p-51-mustang
[14] Australian Air Force, "F-35A specifications — Royal Australian Air Force," Airforce.gov.au, Jun. 14, 2018. https://www.airforce.gov.au/technology/f-35a-specifications
[15] R. Calzada, "P-51D Mustang," NASA, Sep. 08, 2015. https://www.nasa.gov/centers/dryden/multimedia/imagegallery/P-51/P-51_proj_desc.html#: :text=The%20P%2D51D%20was%20the (accessed Jul. 16, 2022)
[16] "Aerospaceweb.org — Aircraft Museum - F-16 Fighting Falcon," Aerospaceweb.org, 2011. http://www.aerospaceweb.org/aircraft/fighter/f16/
[17] "P-51D ROOT (BL17.5) AIRFOIL (p51droot-il)," airfoiltools.com. http://airfoiltools.com/airfoil/details?airfoil=p51droot-il (accessed Jul. 19, 2022).
[18] "NACA 64-206 (naca64206-il)," airfoiltools.com. http://airfoiltools.com/airfoil/details?airfoil=naca64206-il
[19] Mytectutor.com, 2022. https://mytectutor.com/wp-content/uploads/2022/02/Schematic-for-connection-of-L298N-motor-driver-to-Stepper-motor-and-Arduino.png?ezimgfmt=rs:340x230/rscb4 (accessed Jul. 19, 2022).
[20] "ANSYS FLUENT CFD: Supersonic Flow, Oblique Shocks, and Expansion Waves Tutorial," www.youtube.com, Oct. 12, 2017. https://www.youtube.com/watch?v=vB2f-VCa8Lo (accessed Jul. 16, 2022).
[21] "Wave Drag," SKYbrary Aviation Safety, May 26, 2021. https://skybrary.aero/articles/wave-drag#: :text=This%20wave%20drag%20can%%20be (accessed Jul. 21, 2022).